

We call these approaches “top-down” because they start with the observable characteristics induced by a drug and infer the targets based on the likely molecular mechanisms that result in these phenotypes.

On the other hand, bottom-up approaches attempt to learn from chemical properties of proteins or drugs to infer candidate drug–target interactions. For drugs, molecular structure (CITATION GraphDTA), molecular fingerprints, similarity to other drugs (See Bioinf Survey), and other molecular features may be used. On the protein side, secondary structure prediction (CITATION), contact prediction (CITATION), or simply convolution over the amino acid sequences can be used to obtain a feature representation for a given proteins. However, both bottom-up and top-down approaches to drug–target interaction prediction

Don't use “simply”.

replace: “contain and share some problems” with something like “have some limitations”

that are not solvable within themselves.

Following is not sufficiently precise; here, you need to clearly state the challenges faced by both approaches, ideally with references.

Thus, bottom-up approaches share the lack of ability to generalize, which we will show in later sections, and usually focus on engineering sophisticated features for the drugs, while neglecting to formulate meaningful features on the protein side. Top-down approaches lack the ability to spot small differences to cope with small differences within the drug structure and rely heavily on given data for the considered drug–target pair. The latter is not suitable for predictions on novel or unseen compounds, as e.g., data on side effects or its impact on diseases is seldom given for novel drugs.

In order to design such a feature for proteins and drugs, respectively, we make use of the interaction networks for both proteins and compounds. Drug–drug interaction networks were introduced and standardized by Ayvaz et al. (2015) and have been used for clinical decision support (Scheife et al., 2015). Drug–drug interaction networks may give a hint on common targeted pathways. As an additional compound feature we will use semantic side effect similarity, which we will discuss later on.

Generally, try to avoid pointers to “later”.

Protein–protein interaction networks have shown great results in ... ((Vazquez et al., 2003), (Ackerman et al., 2019)) in granting context for molecular system biology. However, these contexts were never applied to the problem of drug–target–interaction prediction. Thus we formalized our hypotheses over these interaction graphs and will test them in the following chapters.

2 Methods

2.1 Problem Description

The issue of predicting drug–target interactions can be described quite briefly: For a given drug and a given protein we want to determine whether those interact or not. We do not differentiate between types of interaction such as activation and inhibition, and do not predict the strength of the interaction. If we additionally make the closed world assumption, i.e., assume that our knowledge is complete and all drug–protein pairs without a known interaction do not interact, we can formulate the problem as a binary classification task.

2.2 Datasets

We obtain a dataset consisting of 12884 human proteins with over 340627 links from STRING (Szklarczyk et al., 2014). For the drug–target interactions, we fetched 229870 links from the STITCH database (Szklarczyk et al., 2015). As both STRING and STITCH provide confidence scores for each association, we filtered them as advised by a threshold of 700, therefore retaining only high-confidence interactions.

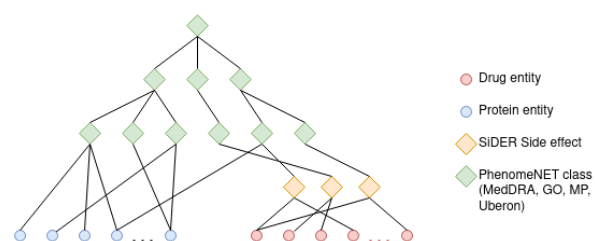


Figure 1. Drugs and proteins with annotations to SIDER and PhenomeNET

We utilize the PhenomeNET ontology (Hoehtendorf et al., 2011), an ontology integrating ontologies such as the Human Phenotype Ontology (Köhler et al., 2018), Gene Ontology (Ashburner et al., 2000; and Seth Carbon et al., 2020), Mammalian Phenotype Ontology (Smith and Eppig, 2009) and several others. We obtained side effects and their links to drugs from SIDER (Kuhn et al., 2015); SIDER contains side effects encoded using identifiers from the MedDRA database (Mozzicato, 2009). We mapped side effects to the PhenomeNET ontology using the *Phenomebrowser.net*, which provides a SPARQL query endpoint for the mentioned resources.

We only use proteins in our analysis that have at least one link in either STITCH or STRING, and drugs with at least one side effect and one existing target. Therefore, the intersection between these resources yields 1,428 drugs and 7,368 human proteins with 32212 interaction links for the training phase. We provide links to and methods for obtaining and processing the necessary data on Github.

For comparative evaluation, we use the gold standard dataset introduced by ? consisting of 1923 interactions between 708 drugs and 1512 proteins.

2.3 Model

Our model combines “top-down” and “bottom-up” information for drug–target identification. We consider an approach to be “top-down” when observable characteristics of either a drug (such as a drug effect) or protein (such as a protein function, or phenotypes resulting from a loss of function) are used to provide information about a molecular mechanisms; we consider an approach “bottom-up” when structural or other molecular information is used to determine a mechanism. In order to build a method that incorporates both top-down and bottom-up features, we first create a model for each type of feature separately. As features for the bottom-up model, we use features derived from molecular structures of drugs from the *SmilesTransformer* (Honda et al., 2019) and molecular features for proteins from *DeepGOPlus* (Kulmanov and Hoehtendorf, 2019). *SmilesTransformer* introduces an autoencoder, learning over the SMILES strings and therefore the molecular organization of each drug in an unsupervised manner. *DeepGOPlus* provides features derived from protein amino acid sequences which are useful to predict protein function.

As phenotypes and functions are encoded through ontologies, we use DL2Vec (Chen et al., 2020) to obtain ontology based representations for use as top-down features. DL2Vec constructs a graph by introducing nodes for each ontology class and edges for ontology axioms, followed by random walks starting from each node in the graph. These walks are encoded using a Word2vec (Mikolov et al., 2013) model. Therefore, DL2Vec generates representations that can encode drug effects or protein functions while preserving their semantic neighbourhood within that graph.

Consider supplement, or combine with other figures.

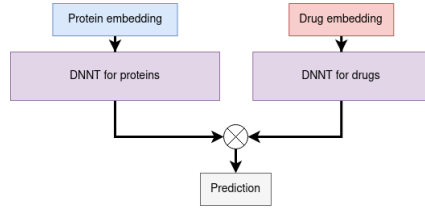


Figure 2. Half-twin network applied to molecular and DL2vec features, utilizing deep learnable feature transformations (LFT). The similarity function \otimes yields the similarity between both transformed embeddings e.g. by computing the cosine similarity.

2.3.1 Half-twin neural networks and modular learnable feature transformation

Looking at the code, I wonder if what is implemented is actually a ANN; it does not look as if the weights are shared between the two networks, so looks more like a twin or half-twin network? Siamese would be $\text{sim}(f(e1), f(e2))$ but the implementation seems to be $\text{sim}(f(e1), g(e2))$.

As we want to learn from the similarity of drug side effects and protein phenotypes, we use a deep half-twin neural network with a contrastive loss using cosine similarity. A half-twin neural network aims to learn a similarity between two embeddings.

Therefore, the precomputed embeddings are run through a regular, neural learnable feature transformation (LFT) network, which also reduces the eventual representation size for drugs and proteins separately. An example structure for both types of features can be found in Figure 2.

While a regular deep neural network, denoted by LFT, for feature space reduction is not particularly novel, we emphasize the versatility of this approach, as both ontology and molecular feature for both drugs and proteins are reduced to similar dimensionality. This allows for a high amount of modularity and different experimental setups by plugging different kinds of features into the model. Additionally, these pretrained features can be used for a variety of other tasks. Additionally, the ontology LFT can be reused for a variety of DL2vec based features with respect to other ontologies and hypotheses. We hereby followed the results of *DL2vec*, indicating that utilizing the activation function $\sigma := \text{LeakyReLU}$ leads to performance increase.

2.3.2 Graph convolutional layers

We included these molecular and ontology-based sub-models with a larger graph convolutional model. The graph underlying the graph convolutional neural network is based on the protein-protein interaction (PPI) graph. The PPI dataset is represented by a graph $G = (V, E)$, where each protein is represented by a vertex $v \in V$, and each edge $e \in E \subseteq V \times V$ symbolizes an interaction between two proteins. Additionally, we introduce a mapping $x : V \rightarrow \mathbb{R}^d$ projecting each vertex v to its node feature $x_v := x(v)$, where d denotes the dimensionality of the node features.

A graph convolutional layer Kipf and Welling (2016) consists of a learnable weight matrix followed by an aggregation step, formalized by

$$\mathbf{X}' = \hat{\mathbf{D}}^{-1/2} \hat{\mathbf{A}} \hat{\mathbf{D}}^{-1/2} \mathbf{X} \Theta \quad (1)$$

where for a given graph $G = (V, E)$, $\hat{\mathbf{A}} = \mathbf{A} + \mathbf{I}$ denotes the adjacency matrix with added self-loops for each vertex, \mathbf{D} is described by $\hat{D}_{ii} = \sum_{j=0} \hat{A}_{ij}$, a diagonal matrix displaying the degree of each node, and Θ denotes the learnable weight matrix. Added self-loops enforce that each node representation is directly dependent on its own preceding one. The number of graph convolutional layers stacked equals the radius of relevant nodes for each vertex within the graph.

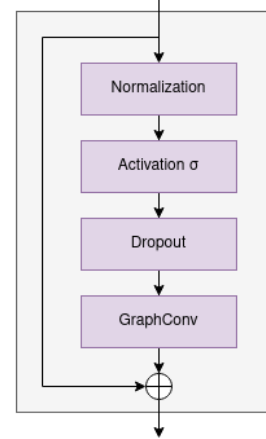


Figure 3. Residual architecture built by Li et al. (2019) and Li et al. (2020b) enabling deeper graph convolutional models

The update rule for each individual node is

$$\mathbf{x}'_i = \Theta \sum_j \frac{1}{\sqrt{\hat{d}_j \hat{d}_i}} \mathbf{x}_j \quad (2)$$

where both \hat{d}_i, \hat{d}_j are dependent on the edge weights e_{ij} of the graph. With simple, single-valued edge weights such as $e_{ij} = 1 \forall (i, j) \in E$, all \hat{d}_i reduce to d_i , i.e., the degree of each vertex i . We denote this type of graph convolutional neural layers with GCNConv.

While in this initial formulation the node-wise update step is defined by the sum over all neighbouring node representations, we are able to alter this formulation to another message passing scheme. We are able to rearrange the order of activation function σ , aggregation AGG and linear neural layer MLP with this formulation as proposed by Li et al. (2020a):

$$\mathbf{x}'_i = \text{MLP}(\mathbf{x}_i + \text{AGG}(\{\sigma(\mathbf{x}_j + \mathbf{e}_{ji}) + \epsilon : j \in \mathcal{N}(i)\})) \quad (3)$$

where we will generally only consider $\sigma \in \{\text{ReLU}, \text{LeakyReLU}\}$. We will denote this generalized layer type as GENConv, following the notation of PyTorch Geometric (Fey and Lenssen, 2019). While the reordering is mainly import for numerical stability, this alteration also addresses the vanishing gradient problem for deeper convolutional networks (Li et al., 2020a). Additionally, we can also generalize the aggregation function to allow different weighting functions such as learnable SoftMax or Power for the incoming signals for each vertex, substituting the averaging step in GCNConv. Hence, while GCNConv suffers from both vanishing gradients and signal fading for large scale, highly connected graphs, each propagation step in GENConv emphasizes signals with values close to 0 and 1. The same convolutional filter and weight matrix are applied to and learned for all nodes simultaneously. We further employ another mechanism to avoid redundancy and fading signals in stacked graph convolutional networks, using residual connections and a normalization scheme (Li et al., 2019, 2020b). The residual blocks are reusable and can be stacked multiple times.

Needs a clearer outline/description/figure of YOUR model structure.

The structure is depicted in Figure 3.

2.3.3 Hyperparameter tuning

As the number of drug-targets are sparse with respect to the number of both drugs and proteins considered, the training, validation and testing

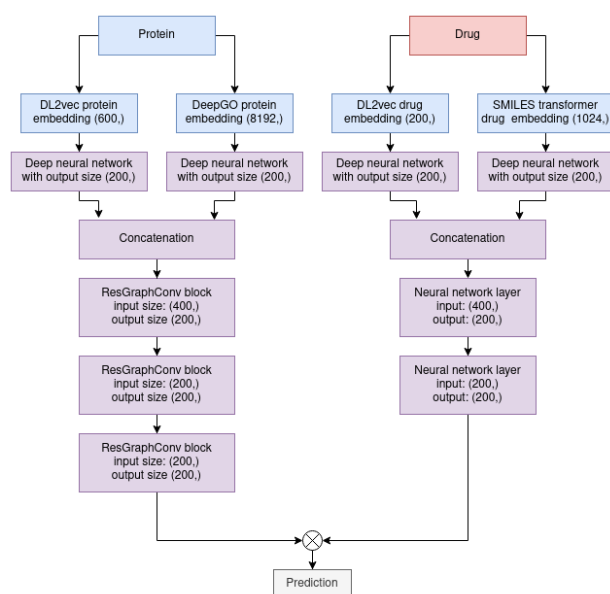


Figure 4. Residual architecture built by Li et al. (2019) and Li et al. (2020b) enabling deeper graph convolutional models

datasets are imbalanced. As there are only 22, 336 links in the considered subset the ratio

$$w := \frac{\#drugs \cdot \#proteins}{\#dti_links} \approx 360, \quad (4)$$

consequently needing compensation in the computed loss function and appropriate metrics for the evaluation.

Therefore, we weighted all positive drug-protein pair samples with this ratio by introducing the following loss function with respect to binary cross-entropy:

$$l(x, y) = -w [y \cdot \log x + (1 - y) \cdot \log(1 - x)] \quad (5)$$

for a given prediction x and target y , and positive weight w defined by equation (4). We average this loss among all drug-protein pairs in the training set, leading to a stable environment for the used optimizing scheme *Adam* (Kingma and Ba, 2014). We implemented a 5-fold cross validation split among the proteins. Furthermore, we used early stopping in the training process for optima detection.

To find the best hyperparameter configuration for the proposed model we performed a grid search to find the most expressive and non-redundant representation. We pretrained the bottom-up and the top-down model separately and aimed at best performing models with respect to our evaluation metrics. We optimized embedding sizes, depth of the neural network, optimizer, learning rate and layer types using an extensive, manual grid search. Starting from naïve, shallow feature transformations with an embedding size of 10, we scaled the network up to residual structures with up to 10 hidden layers leading to embeddings of size 4000, testing different network widths and learning rates for each configuration.

2.4 Evaluation and metrics

To assess each model, we compute a variety of common metrics for binary classification. As the datasets are highly imbalanced, we use the area under the receiver operating characteristic curve (AUROC) on training, validation and testing split.

We calculate the AUROC by computing true positive rate at various false positive rate thresholds and using trapezoidal approximations

to estimate the area under the curve. We refer to this measure as *MacroAUC*.

For RH: check this again later:

In contrast we also calculate the *MicroAUC* score. For given lists D, P of drugs and proteins, respectively, and a set of known interactions $Int := \{(d_i, p_i)\}$, *MicroAUC* is calculated as the average per entity (macro) *AUROC* score. With respect to proteins, this can be formalized for given labels $l : D \times P \rightarrow \{0, 1\}$ and predictions $y : D \times P \rightarrow [0, 1]$ as

$$MicroAUC_p := \frac{mean}{p \in P} (\{AUROC(\{(l(d_i, p), y(d_i, p)) | d_i \in D\})\})$$

Drugs and proteins can be interchanged in this formulation, while we refer to the different measures as protein-centric microAUC (*MicroAUC_p*) and a drug-centric microAUC (*MicroAUC_d*). Additionally, the *MicroAUC* score may not be defined as in some datasets some targets or drugs, respectively, do not have any interactions, leading to an infeasible $TPR = 0$ for all thresholds and an undefined *AUROC* score for that entity. For those entities we impute the *MicroAUC* interpolating linearly, by using the accuracy for this subset.

3 Results

3.1 Voodoo : computational model to identify drugs that target a protein

Within DTI prediction, there are potential biases resulting from the underlying datasets (Pahikkala et al., 2014). First, novel drugs are often designed by altering non-functional components of a drug, leading to two and more very similar drugs designed to target the same proteins (Overington et al., 2006). This can result in a bias when it leads to hidden duplicates that can distribute among the train/test split, resulting in a better (measured) predictive performance than would be expected when the model is applied to identify drugs that target a protein for which no drugs yet exist. Second, some proteins (which we will denote as *hub proteins*) have significantly more known interactions with drugs than others. In the STITCH database,

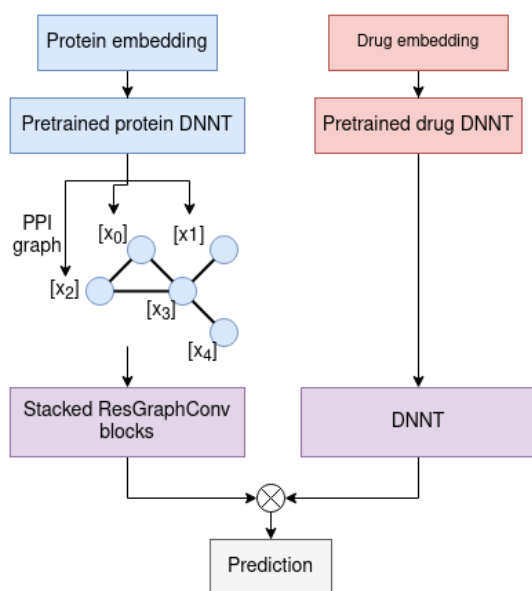


Figure 5. Full DTI prediction model based on the pretrained learnable feature transformations (LFT) for either molecular structure or ontology based features. The transformed protein representations are added to each corresponded protein as node features for the graph convolutional steps.

5% of the proteins have 40% of the interactions, and similar distributions are present in the Yamanishi and Drugbank datasets (Wishart *et al.*, 2007, 2017) datasets; preferentially predicting these proteins may increase predictive performance while again not reflecting the actual performance when applied to a new protein (e.g., a protein for which no interactions are known). These differences in the number of drugs targeting certain proteins may be the result of study bias where more “valuable” proteins have more drugs designed to target them due to their involvement in more common diseases (or diseases for which drugs can be more profitably marketed).

We developed Voodoo as a computational model to predict drug–target interactions. Specifically, given a protein, Voodoo will identify and rank known drugs that likely target this protein. Voodoo combines two types of features: structural information for drugs and proteins that can be used to determine if they may physically interact, and information about drug effects that may localize on an interaction network. As structural features, Voodoo uses structural representations of drugs from the SMILES transformer (Honda *et al.*, 2019) and representations of protein amino acid sequences from DeepGOPlus (Kulmanov and Hoehndorf, 2019). Voodoo learns representations of drug effects and protein functions using the ontology-based machine learning method DL2Vec (Chen *et al.*, 2020).

Move to methods:

When combining ontology and molecular features with or without the graph model, we concatenate both protein features and both drugs features, before plugging them into the graph or the similarity computation.

We use two half-twin neural networks to combine the molecular and phenotype representations of drugs and proteins, and add these to a protein interaction network as node labels. We then train this model in an end-to-end manner using a graph neural network architecture. The overall workflow is depicted in Figure 5.

We first perform a cross-validation over proteins and validate our results. Cross-validation over proteins aims to evaluate how the model

make sure it's a workflow

STITCH results	PPI graph			
	without	with	without	with
	AUROC	Micro AUC_p	AUROC	Micro AUC_p
MolPred	0.69	0.65	0.69	0.67
OntoPred	0.88	0.87	0.92	0.93
MolPred + Onto-Pred	0.89	0.90	0.93	0.94

Yamanishi results	PPI graph			
	without	with	without	with
	AUROC	Micro AUC	AUROC	Micro AUC_p
MolPred + Onto-Pred	0.83	0.82	0.84	0.84

Figure 6. Results for Voodoo on STITCH and Yamanishi dataset evaluated with a 5-fold cross-validation. MolPred and OntoPred are the predictors for molecular and ontology based features, respectively.

performs when tasked to identify drugs that may target a “novel” protein, i.e., one not seen during training.

Describe/add the CV results here.

Second, we use the model trained on STITCH and evaluate the model on the Yamanishi benchmark dataset.

Maybe remove microAUC here, introduce in next section?

We trained, validated and finally tested all considered models on the STITCH dataset using a 5-fold cross-validation over a protein split; we then selected the best-performing models (with respect to $AUROC$ and $MicroAUC_p$) and evaluate them on the Yamanishi benchmark dataset. To evaluate the influence of the different features separately, and determine whether they “localize” on the PPI graph (and therefore can be exploited successfully by the graph neural networks), we train and evaluate models with different types of features, and with and without inclusion of the PPI graph, separately. Table 6 shows the results.

Move to caption of table.

We will hereby denote the molecular feature based predictor with *MolPred*, while abbreviating the ontology based, top-down predictor with *OntoPred*.

We find that the model using ontology-based features (*OntoPred*) is showing significantly better performance on STITCH compared to using only molecular features. We also observe that only the model using ontology-based features results in significantly increased performance when incorporating the PPI graph. This increase can be observed with different graph neural network architectures. While the *GCNConv* and *GENConv* architecture already shows an improvement, the *ResGraphConv* blocks add a large amount of additional learnable parameters to the network, leading to more expressive power. To test whether the improvement is due to the number of learnable parameters added or the result of better exploiting the information about PPIs, we experiment with a graph model in which all graph convolutional neural layers in the residual blocks are removed. This pruned network, with no information on the protein–protein interactions, reached very similarly results as the original *OntoPred* model and showed no improvement.

Not clear, need to reformulate:

Furthermore, when substituting the original *GENConv* layers with *GCNConv* or other related layers in the graph convolutional step of the *ResGraphConv* blocks, this model would achieve once again no significant performance gain in comparison to the plain *OntoPred* one. This performance increase was only noticeable for *GENConv* layers. The discrepancy

This needs another sentence stating how you made sure there was no overlap in data.

significance test and p value? otherwise remove

p-val

data not in the table

is this still a graph model?

data not shown; and details missing from Methods

of *GENConv* and *GCNConv* may be founded in numerical stability and fading signals, as described in the introduction of both methods.

p val As the inclusion of graph information significantly increases performance, we conclude that information about protein functions localizes on the graph while molecular features do not.

3.2 Protein-centric evaluation

The goal of Voodoo is to find candidate drugs that target a specific protein; however, our evaluation does not evaluate this application but rather how Voodoo would perform in finding plausible drug–target interactions among all possible interactions. To provide a better estimate on how Voodoo performs for individual protein targets, we use micro-averages between proteins and compute the *MicroAUC*; micro-averages average the performance (true and false positive rates) per protein instead of across all drug–protein pairs.

Furthermore, we hypothesize that some of the predictions made by our model are the result of the biases in drug–target interaction datasets. We design a “naïve” baseline model that predicts the same list of proteins for each drugs based on the number of known drug–target interactions for a protein. Formally, given lists *D* and *P* of drugs and proteins and a set of known interactions $\mathcal{I} := \{(d_i, p_i)\}$, we construct an interaction matrix $M_{int} \in \{0, 1\}^{|D| \times |P|}$ with

$$M_{ij} = \begin{cases} 1 & \text{if } (d_i, p_j) \in \mathcal{I} \\ 0 & \text{otherwise} \end{cases}$$

describing for all drug–protein pairs whether there is a known interaction or not. We now rank all proteins $p_j \in P$ descending by their number of drug interactors by summing over the columns of M_{ij} and ranking these sums:

$$f : P \rightarrow \mathbb{N} \text{ with } f : p_j \mapsto \sum_{i=1}^{|D|} M_{ij}$$

Our “naïve” predictor P_k predicts all drugs to interact with the top *k* targets with respect to the introduced ranking:

$$P_k : D \times P \rightarrow \{0, 1\} \text{ with } P_k : d_i, p_j \mapsto \begin{cases} 1 & \text{if } p_j \in Top_k(P) \\ 0 & \text{otherwise} \end{cases}$$

with the only hyperparameter *k*. The prediction P_k is not dependent on the drug d_i and will predict the same ranked list of drugs for a given protein p_j ; consequently, this naïve predictor does not predict any useful information about interactions between drugs and proteins.

We apply this naïve predictor on both the STITCH and Yamanishi datasets, using the full dataset as well as 5-fold cross-validation over drugs and drug–protein pairs. For each fold, we gradually increase *k*, eventually saving the best performance for each fold. Using the full dataset, drug–target split, and drug split, we obtain

are these micro or macro AUC?

merge table results in text

Dataset	Splitting scheme		
	Whole	DT pairs	Drugs
STITCH	0.76	0.70	0.73
Yamanishi	0.88	0.84	0.85

p-val The baseline predictor shows significantly higher performance than a random classifier on both datasets, with better results on the Yamanishi benchmark.

For comparison with the state of the art methods, we chose the best performing methods for drug–target interaction prediction that were previously evaluated on the Yamanishi benchmark dataset. These state-of-the-art methods approaches include DTIGEMS+ (Thafar et al., 2020) and

Approach	Original scheme		Protein split	
	Splitting scheme	AUROC score	AUROC score	Micro AUC_p
DTINet	DP pairs	0.91	0.84	0.67
DTIGEMS+	DP pairs	0.93	0.72	0.68
DTI-CDF	Proteins	0.86	0.85	0.79

Approach	Original scheme		Protein split	
	Splitting scheme	AUROC score	AUROC score	Micro AUC_p
DeepDTI	Drugs	0.88	0.76	0.70
DeepDTA	DP pairs	0.88	0.77	0.69
DeepConv-DTI	DP pairs	0.88	0.76	0.73
MolTrans	DP pairs	0.90	0.77	0.74

Figure 7. Test

DTI-CDF (Chu et al., 2019), which have showed superior results in comparison to numerous works. Furthermore, we added DTINet (Luo et al., 2017) as method for comparison which has been used to develop a number of methods such as NeoDTI (Wan et al., 2019) with similar methodology.

We evaluate all models on their recommended splitting scheme choice, hyperparameters and folds in cross-validation, measuring their respective AUROC. We further evaluate each model by performing a protein-wise cross-validation determining (macro) AUROC and *MicroAUC_p*. For this evaluation we allow stratification for the training process but not for the validation and testing phase as real world applications of these models would have to deal with imbalanced data.

Merge the tables; add Voodoo model to table to allow DIRECT comparison:

The results of the analysis are summarized in the upper part of Figure 7.

We find that...
summarize key findings from Table.
Replace/merge table:
Discussion:

The lack of stratification, only impacts the not considered area under precision recall curve (AUPRC) and not the Macro AUROC score, while also supporting the expressiveness of *MicroAUC_p* with more data points.

4 Discussion

Methods:
Through the very nature of the graph convolutional neural network, we build the transformed representation for all proteins in every forwarding step of the model. Note particularly, that the same convolutional filter and weight matrix are applied to and learned for all nodes simultaneously. By construction, for a single drug we can compute and predict all its interactors in a single run of the model, leading to significantly less computing time.
Likely discussion:

The aim of Voodoo is to predict candidate drugs that target a given protein; the challenge is to develop a training and evaluation scheme that does not simply overfit to the inherent biases in training and testing data. In general, when performing cross-validation for DTI prediction, the options are to split over

- 1. split over drugs,
- 2. split over drug–target pairs, or
- 3. split over proteins

where the first and third option concern splitting drugs and proteins, respectively, into train, validation and test sets, and arranging the corresponding drug-target interactions. They ensure that at least parts of the interactions are not seen during training and evaluate either how well targets are predicted for unseen drugs or unseen proteins. Hereby, different training and prediction schemes lead to divergent expressiveness of the resulting model.

Likely discussion:

The most common scheme for DTI prediction is the split over drug-target pairs (Wang and Kurgan, 2018), where likely all drugs and targets of the validation and testing phase have already occurred in the training phase, as part of other drug-target pairs. The second most prevalent arrangement is the split over drugs, while only close to none is aiming on a protein split. However, the first and second splitting scheme are exposed to the first dataset bias and are hence more likely vulnerable to transductive inference by just predicting recently seen structures, rather than implementing inductive inference and generalizing over the drug representations. Second, these two strategies are more susceptible to the second bias, as only in these cases the model may overfit on the number of existing interactions for a single protein, while in the third scheme the number of interactions of the test proteins is entirely unknown during training process.

Likely discussion:

Assuming a hypothetical, perfectly generalizing model built upon an unbiased dataset, this very model would yield similar performances for all three splitting schemes, not overfitting on the known structures. On the other hand, for a hypothetical entirely overfitting model, trained on a highly biased dataset, this model would show substantial deviations from the original performance over another split.

Likely discussion:

We emphasize, that all real-world models are prone to some sort of overfitting, and unknown, deviant entities in both validation and testing set will likely lead to some sort of performance gap for relevant metrics. However, a large disparity may hint the biases stated above.

Approach	Splitting scheme	Original AUROC score	Protein split AUROC	MicroAUC
DeepDTI	Drugs	87.6	75.9	70.1
DeepDTA	DP pairs	87.6	76.7	69.4
DeepConv-DTI	DP pairs	88.3	76.6	73.0
MolTrans	DP pairs	89.5	77.0	74.0

4.1 Deification of our method

- we built protein function and ontology based features based on DL2vec
- Ontology derived protein function focused features are highly predictive for dtis
- We built a versatile template for various features to test localization on the PPI graph
- normal GCNs don't work on PPI graph, as it is highly connected → needs stronger more expressive aggregation function → GENConv in residual blocks for better numerical stability
- protein functions localize on the PPI graph, while molecular features don't
- all AUROC in % AUROC score on STITCH

DNNT model	Without graph model	With graph model
MolPred	69	69
PhenomeNETPred	88	92
MolPred + PhenomeNETPred	89	93

- microAUC for MolPred + PhenomeNETPred on graph is about 93 + –
- and on yamanishi dataset

DNNT model	Without graph model	With graph model
PhenomeNETPred	83	84
MolPred + PhenomeNETPred	83	84.5

- MicroAUC is about 83

4.2 How to insult other methods

- Only few other methods perform their split over proteins (Wang and Kurgan, 2018), DTI-CDF does it

- Running split over proteins is harder than, drug and drug protein pair split (see below table)
- this applies for both DTI prediction and drug target affinity prediction (and Saras gene-disease association)
- using indications is like cheating, as not applicable for searching new drugs
- drug indications are highly predictive for downstream tasks, but lack capability to differentiate highly related drugs/proteins
- Stratified Cross validation is suitable for training, but **NOT** for validating and testing (Uselessly high AUPRC)
- microAUC is a superior and more intuitive metric for drug repurposing → why for each protein and not for each drug

Approach	Splitting scheme	Original AUROC score	Protein split AUROC	MicroAUC
DTINet	DP pairs	91	84.1	67.2
DTIGEMS+	DP pairs	93	72.2	67.8
DTI-CDF	Proteins	83	83	79

- A naive predictor (ranking proteins) and predict each drug similarly achieves cutting edge performance (87.5 AUROC for whole dataset, 85.5 for 5-fold cross validation in drug-split) → No prot focused microAUC possible. → hub proteins
- Yamanishi Dataset is only partially suitable , if everybody just derives a suitable subset (DTIGEMS)
- This also applies to drug target affinity prediction. We were hereby able to roughly reproduce the results from MolTrans (Bioinformatics) on BioSnap

for comparing results

4.3 Tested hypotheses

In this work we are testing the following hypotheses:

1. Can we build a model that outperforms state of the art approaches, combining top-down and bottom-up approaches?
2. Are interaction networks sufficient to improve the performance of simple molecular predictors?

We will test the first hypothesis by building a model that takes both top-down and bottom-up features into account. Thus, we propose a novel approach to combine those mutual exclusive attempts, through the usage of interaction networks, similarity and molecular features. Additionally, we test the latter by building a simple molecular DTI predictor and enhance it under usage of the interaction networks.

For the bottom-up approach we build a model that only relies on molecular features, which we will discuss in more detail in the following methods chapter. For the combination of both approaches we now attach the predictions to the protein-protein interaction graph as node features for future graph learning steps. In this graph we tried to find both patterns and regions for each drug that could be of interest through application of different graph convolutional layers, which in return represent the feature for each protein. Representing the drug we take the drug-drug interaction graph and the semantic similarity over side effects which we will explain in the following paragraphs.

5 Methods

5.1 Models

The used model consists of two separate models, that help to fuse together the two methods:

1. The molecular predictor
2. The interaction network based predictor

We build the molecular predictor by using pretrained, molecular fingerprints models for both drugs and proteins. Regarding proteins, we used the pretrained feature generator from *DeepGoPlus* ((Kulmanov and Hoehndorf, 2019)) that was originally designed for protein function prediction and is regarded as state of the art for this purpose. For drugs we used a pretrained fingerprint model from *SMILES transformer* ((Honda et al., 2019)), that provides a simple and fast method to compute fingerprints through autoencoder models. The encodings from these two models were funneled into a simple deep neural network (see Figure ??) with few fully connected.

The results of that prediction flow into the annotation of the protein-protein interaction (PPI) graph as depicted in (IMAGE). Hereby, the predictions of the molecular predictor are used as node features for the graph, with respect to the given drug. Thus, given a compound-target pair, the nodes of the PPI graph now hold bottom-up features, which can now be processed by the graph learning algorithms.

The PPI graph is processed by different graph convolutional layers, that may underline the importance of either patterns or regions within the graph, to obtain a feature vector for the wanted node. In contrast to learning over whole graphs we perform node classification within the graph. These layers are either graph convolutional layers, that learn a certain kernel over the graph, or attention based. Different layers of both and other types such as were tested.

The drug-drug interaction features are retrieved by choosing the corresponding row in the adjacency matrix of the graph, thus leading to quite simple features.

For the semantic similarity feature, that once again represents a top-down

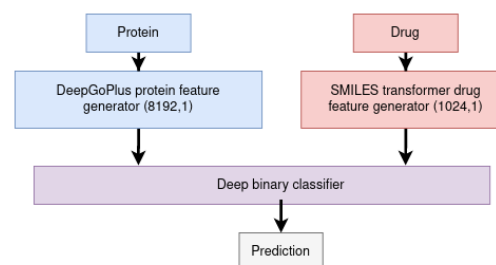


Figure 8. Molecular predictor based on the generated features from DeepGoPlus and SMILES transformer.

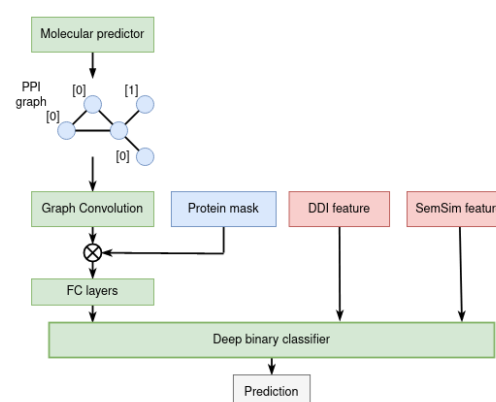


Figure 9. Deep neural network that predicts based on drug-drug interaction features and semantic similarity features over side effects for drugs, and graph convolution over protein-protein interaction networks for proteins. Protein and drug features are represented by blue and red, respectively.

attribute, we artificially link each drug to its corresponding side effects in the MedDRA hierarchy. Concerning this hierarchy, drug-drug similarity is computed by the Resnik similarity ((Resnik, 1995)). For the given compound we take the corresponding row of this symmetric similarity matrix.

Thereby, we concatenate these three features together and funnel them into another deep neural network as depicted in figure 9. This network finally yields our prediction. We hereby perform splits over both drugs and proteins, in order to test and show the discrepancy and increasing difficulty.

Implementation was done in PyTorch ((Paszke et al., 2019)) and is available on Github under github.com/thinnerichs/KAUST-dti-metabol. Graph learning methods were build with help of PyTorch-Geometric ((Fey and Lenssen, 2019)), a geometric deep learning extension library for PyTorch, that recently got a lot of attention in the machine learning community. This library gives the potential to use many state of the art graph learning mechanisms, such as plain but effective graph convolution (Kipf and Welling (2016)), Chebychev kernels ((Defferrard et al., 2016)), ARMA kernels ((Bianchi et al., 2019)), translation-invariant operators ((Verma et al., 2017)), attention mechanisms ((Veličković et al., 2017)), random walks ((Klicpera et al., 2018)) and mixtures of the latter two ((Hamilton et al., 2017)). The performance of these various layer types were tested for this particular problem, as discussed in the results section.

6 Discussion

7 Conclusion
Acknowledgements

This work has been supported by the... Text Text Text Text.

References

Ackerman, E. E., Alcorn, J. F., Hase, T., and Shoemaker, J. E. (2019). A dual controllability analysis of influenza virus-host protein-protein interaction networks for antiviral drug target discovery. *BMC Bioinformatics*, **20**(1).

and Seth Carbon, Douglass, E., Good, B. M., Unni, D. R., Harris, N. L., Mungall, C. J., Basu, S., Chisholm, R. L., Dodson, R. J., Hartline, E., Fey, P., Thomas, P. D., Albou, L.-P., Ebert, D., Kesling, M. J., Mi, H., Muruganujan, A., Huang, X., Mushayahama, T., LaBonte, S. A., Siegele, D. A., Antonazzo, G., Attrill, H., Brown, N. H., Garapati, P., Marygold, S. J., Trovisco, V., dos Santos, G., Falls, K., Tabone, C., Zhou, P., Goodman, J. L., Strelets, V. B., Thurmond, J., Garmiri, P., Ishtiaq, R., Rodríguez-López, M., Acencio, M. L., Kuiper, M., Lægreid, A., Logie, C., Lovering, R. C., Kramarz, B., Saverimuttu, S. C. C., Pinheiro, S. M., Gunn, H., Su, R., Thurlow, K. E., Chibucos, M., Giglio, M., Nadendla, S., Munro, J., Jackson, R., Duesbury, M. J., Del-Toro, N., Meldal, B. H. M., Paneerselvam, K., Perfetto, L., Porras, P., Orchard, S., Shrivastava, A., Chang, H.-Y., Finn, R. D., Mitchell, A. L., Rawlings, N. D., Richardson, L., Sangrador-Vegas, A., Blake, J. A., Christie, K. R., Dolan, M. E., Drabkin, H. J., Hill, D. P., Ni, L., Sitnikov, D. M., Harris, M. A., Oliver, S. G., Rutherford, K., Wood, V., Hayles, J., Bähler, J., Bolton, E. R., Pons, J. L. D., Dwinell, M. R., Hayman, G. T., Kaldunski, M. L., Kwitek, A. E., Laulederkind, S. J. F., Plasterer, C., Tutaj, M. A., Vedi, M., Wang, S.-J., D'Eustachio, P., Matthews, L., Balhoff, J. P., Aleksander, S. A., Alexander, M. J., Cherry, J. M., Engel, S. R., Gondwe, F., Karra, K., Miyasato, S. R., Nash, R. S., Simison, M., Skrzypek, M. S., Weng, S., Wong, E. D., Feuermann, M., Gaudet, P., Morgat, A., Bakker, E., Berardini, T. Z., Reiser, L., Subramaniam, S., Huala, E., Arighi, C. N., Auchincloss, A., Axelsen, K., Argoud-Puy, G., Bateman, A., Blatter, M.-C., Boutet, E., Bowler, E., Breuza, L., Bridge, A., Britto, R., Bye-A-Jee, H., Casas, C. C., Coudert, E., Denny, P., Estreicher, A., Famiglietti, M. L., Georghiou, G., Gos, A., Gruaz-Gumowski, N., Hatton-Ellis, E., Hulo, C., Ignatchenko, A., Jungo, F., Laiho, K., Mercier, P. L., Lieberherr, D., Lock, A., Lussi, Y., MacDougall, A., Magrane, M., Martin, M. J., Masson, P., Natale, D. A., Hyka-Nouspikel, N., Orchard, S., Pedruzzi, I., Pourcel, L., Poux, S., Pundir, S., Rivoire, C., Speretta, E., Sundaram, S., Tyagi, N., Warner, K., Zaru, R., Wu, C. H., Diehl, A. D., Chan, J. N., Grove, C., Lee, R. Y. N., Muller, H.-M., Raciti, D., Auken, K. V., Sternberg, P. W., Berriman, M., Paulini, M., Howe, K., Gao, S., Wright, A., Stein, L., Howe, D. G., Toro, S., Westerfield, M., Jaiswal, P., Cooper, L., and Elser, J. (2020). The gene ontology resource: enriching a GOLD mine. *Nucleic Acids Research*, **49**(D1), D325–D334.

Ashburner, M., Ball, C. A., Blake, J. A., Botstein, D., Butler, H., Cherry, J. M., Davis, A. P., Dolinski, K., Dwight, S. S., Eppig, J. T., Harris, M. A., Hill, D. P., Issel-Tarver, L., Kasarskis, A., Lewis, S., Matese, J. C., Richardson, J. E., Ringwald, M., Rubin, G. M., and Sherlock, G. (2000). Gene ontology: tool for the unification of biology. *Nature Genetics*, **25**(1), 25–29.

Ayvaz, S., Horn, J., Hassanzadeh, O., Zhu, Q., Stan, J., Tatonetti, N. P., Vilar, S., Brochhausen, M., Samwald, M., Rastegar-Mojarad, M., Dumontier, M., and Boyce, R. D. (2015). Toward a complete dataset of drug–drug interaction information from publicly available sources. *Journal of Biomedical Informatics*, **55**, 206–217.

Bianchi, F. M., Grattarola, D., Alippi, C., and Livi, L. (2019). Graph neural networks with convolutional arma filters.

Chen, J., Althagafi, A., and Hoehndorf, R. (2020). Predicting candidate genes from phenotypes, functions and anatomical site of expression. *Bioinformatics*.

Chu, Y., Kaushik, A. C., Wang, X., Wang, W., Zhang, Y., Shan, X., Salahub, D. R., Xiong, Y., and Wei, D.-Q. (2019). DTI-CDF: a cascade deep forest model towards the prediction of drug-target interactions based on hybrid features. *Briefings in Bioinformatics*, **22**(1), 451–462.

Defferrard, M., Bresson, X., and Vandergheynst, P. (2016). Convolutional neural networks on graphs with fast localized spectral filtering.

Fey, M. and Lenßen, J. E. (2019). Fast graph representation learning with Py-Torch Geometric. In *ICLR Workshop on Representation Learning on Graphs and Manifolds*.

Hamilton, W. L., Ying, R., and Leskovec, J. (2017). Inductive representation learning on large graphs.

Hoehndorf, R., Schofield, P. N., and Gkoutos, G. V. (2011). PhenomeNET: a whole-phenome approach to disease gene discovery. *Nucleic Acids Research*, **39**(18), e119–e119.

Honda, S., Shi, S., and Ueda, H. R. (2019). Smiles transformer: Pre-trained molecular fingerprint for low data drug discovery.

Kingma, D. P. and Ba, J. (2014). Adam: A method for stochastic optimization.

Kipf, T. N. and Welling, M. (2016). Semi-supervised classification with graph convolutional networks.

Klicpera, J., Bojchevski, A., and Günnemann, S. (2018). Predict then propagate: Graph neural networks meet personalized pagerank.

Köhler, S., Carmody, L., Vasilevsky, N., Jacobsen, J. O. B., Danis, D., Gouridine, J.-P., Gargano, M., Harris, N. L., Matentzoglou, N., McMurtry, J. A., Osumi-Sutherland, D., Cipriani, V., Balhoff, J. P., Conlin, T., Blau, H., Baynam, G., Palmer, R., Gratian, D., Dawkins, H., Segal, M., Jansen, A. C., Muaz, A., Chang, W. H., Bergerson, J., Laulederkind, S. J. F., Yüksel, Z., Beltran, S., Freeman, A. F., Sergouniotis, P. I., Durkin, D., Storm, A. L., Hanauer, M., Brudno, M., Bello, S. M., Sincan, M., Rageth, K., Wheeler, M. T., Oegema, R., Loughi, H., Rocca, M. G. D., Thompson, R., Castellanos, F., Priest, J., Cunningham-Rundles, C., Hegde, A., Lovering, R. C., Hajek, C., Olry, A., Notarangelo, L., Similuk, M., Zhang, X. A., Gómez-Andrés, D., Lochmüller, H., Dollfus, H., Rosenzweig, S., Marwaha, S., Rath, A., Sullivan, K., Smith, C., Milner, J. D., Leroux, D., Boerkoel, C. F., Klion, A., Carter, M. C., Groza, T., Smedley, D., Haendel, M. A., Mungall, C., and Robinson, P. N. (2018). Expansion of the human phenotype ontology (HPO) knowledge base and resources. *Nucleic Acids Research*, **47**(D1), D1018–D1027.

Kuhn, M., Letunic, I., Jensen, L. J., and Bork, P. (2015). The SIDER database of drugs and side effects. *Nucleic Acids Research*, **44**(D1), D1075–D1079.

Kulmanov, M. and Hoehndorf, R. (2019). DeepGOPlus: improved protein function prediction from sequence. *Bioinformatics*.

Li, G., Müller, M., Thabet, A., and Ghanem, B. (2019). Deepgcns: Can gcns go as deep as cnns?

Li, G., Xiong, C., Thabet, A., and Ghanem, B. (2020a). Deeppergcn: All you need to train deeper gcns.

Li, G., Xiong, C., Thabet, A., and Ghanem, B. (2020b). Deeppergcn: All you need to train deeper gcns.

Luo, Y., Zhao, X., Zhou, J., Yang, J., Zhang, Y., Kuang, W., Peng, J., Chen, L., and Zeng, J. (2017). A network integration approach for drug-target interaction prediction and computational drug repositioning from heterogeneous information.

Mikolov, T., Chen, K., Corrado, G., and Dean, J. (2013). Efficient estimation of word representations in vector space.

Mozzicato, P. (2009). MedDRA. *Pharmaceutical Medicine*, **23**(2), 65–75.

Overington, J. P., Al-Lazikani, B., and Hopkins, A. L. (2006). How many drug targets are there? *Nature Reviews Drug Discovery*, **5**(12), 993–996.

Pahikkala, T., Airola, A., Pietila, S., Shakyawar, S., Sz wajda, A., Tang, J., and Aittokallio, T. (2014). Toward more realistic drug-target interaction predictions. *Briefings in Bioinformatics*, **16**(2), 325–337.

Paszke, A., Gross, S., Massa, F., Lerer, A., Bradbury, J., Chanan, G., Killeen, T., Lin, Z., Gimelshein, N., Antiga, L., Desmaison, A., Kopf, A., Yang, E., DeVito, Z., Raison, M., Te jani, A., Chilamkurthy, S., Steiner, B., Fang, L., Bai, J., and Chintala, S. (2019). Pytorch: An imperative style, high-performance deep learning library. In H. Wallach, H. Larochelle, A. Beygelzimer, F. d'Alché-Buc, E. Fox, and R. Garnett, editors, *Advances in Neural Information Processing Systems 32*, pages 8024–8035. Curran Associates, Inc.

Resnik, P. (1995). Using information content to evaluate semantic similarity in a taxonomy.

Scheife, R. T., Hines, L. E., Boyce, R. D., Chung, S. P., Momper, J. D., Sommer, C. D., Abernethy, D. R., Horn, J. R., Sklar, S. J., Wong, S. K., Jones, G., Brown, M. L., Grizzle, A. J., Comes, S., Wilkins, T. L., Borst, C., Wittie, M. A., and Malone, D. C. (2015). Consensus recommendations for systematic evaluation of drug–drug interaction evidence for clinical decision support. *Drug Safety*, **38**(2), 197–206.

Smith, C. L. and Eppig, J. T. (2009). The mammalian phenotype ontology: enabling robust annotation and comparative analysis. *Wiley Interdisciplinary Reviews: Systems Biology and Medicine*, **1**(3), 390–399.

Szklarczyk, D., Franceschini, A., Wyder, S., Forslund, K., Heller, D., Huerta-Cepas, J., Simonovic, M., Roth, A., Santos, A., Tsafou, K. P., Kuhn, M., Bork, P., Jensen, L. J., and von Mering, C. (2014). STRING v10: protein–protein interaction networks, integrated over the tree of life. *Nucleic Acids Research*, **43**(D1), D447–D452.

Szklarczyk, D., Santos, A., von Mering, C., Jensen, L. J., Bork, P., and Kuhn, M. (2015). STITCH 5: augmenting protein–chemical interaction networks with tissue and affinity data. *Nucleic Acids Research*, **44**(D1), D380–D384.

Thafar, M. A., Olayan, R. S., Ashoor, H., Albaradei, S., Bajic, V. B., Gao, X., Gojobori, T., and Essack, M. (2020). DTiGEMS: drug-target interaction prediction using graph embedding, graph mining, and similarity-based techniques. *Journal of Cheminformatics*, **12**(1).

Vazquez, A., Flammini, A., Maritan, A., and Vespignani, A. (2003). Global protein function prediction from protein-protein interaction networks. *Nature Biotechnology*, **21**(6), 697–700.

Veličković, P., Cucurull, G., Casanova, A., Romero, A., Liò, P., and Bengio, Y. (2017). Graph attention networks.

picture(0,0)(-35,0)(1,0)30 (0,35)(0,-1)30 picture

picture(0,0)(35,0)(-1,0)30 (0,35)(0,-1)30 picture

Verma, N., Boyer, E., and Verbeek, J. (2017). Feastnet: Feature-steered graph convolutions for 3d shape analysis.

Wan, F., Hong, L., Xiao, A., Jiang, T., and Zeng, J. (2019). NeoDTI: neural integration of neighbor information from a heterogeneous network for discovering new drug–target interactions. *Bioinformatics*, **35**(1), 104–111.

Wang, C. and Kurgan, L. (2018). Review and comparative assessment of similarity-based methods for prediction of drug–protein interactions in the druggable human proteome. *Briefings in Bioinformatics*, **20**(6), 2066–2087.

Wishart, D. S., Knox, C., Guo, A. C., Cheng, D., Shrivastava, S., Tzur, D., Gautam, B., and Hassanali, M. (2007). DrugBank: a knowledgebase for drugs, drug actions and drug targets. *Nucleic Acids Research*, **36**(suppl_1), D901–D906.

Wishart, D. S., Feunang, Y. D., Guo, A. C., Lo, E. J., Marcu, A., Grant, J. R., Sajed, T., Johnson, D., Li, C., Sayeeda, Z., Assempour, N., Iynkkaran, I., Liu, Y., Maciejewski, A., Gale, N., Wilson, A., Chin, L., Cummings, R., Le, D., Pon, A., Knox, C., and Wilson, M. (2017). DrugBank 5.0: a major update to the DrugBank database for 2018. *Nucleic Acids Research*, **46**(D1), D1074–D1082.

picture(0,0)(-35,0)(1,0)30 (0,-35)(0,1)30 picture

picture(0,0)(35,0)(-1,0)30 (0,-35)(0,1)30 picture